International Journal of Research in Engineering, Science and Management
Volume 5, Issue 1, January 2022
https://www.ijresm.com | ISSN (Online): 2581-5792

Application of Resistivity Survey Method in Vellar River Basin, Cuddalore District, Tamilnadu, India

R. Rajasekar[1*], K. Sankar[2], D. Santhi[3], B. Karthik[4], R. Suresh[5], T. Manivel[6]
[1,2,3,4]*Department of Industries and Earth Sciences, Tamil University, Thanjavur, India*
[5,6]*Department of Earth Sciences, Annamalai University, Annamalinagar, Chidambaram, India*

***Abstract*: In the present study, an attempt was made to prepare vertical pseudo section of resistivity and generate possible resistivity models of the study area. Besides, the pseudo sections will facilitate understanding the variations of subsurface lithology and helpful to delineate potential freshwater aquifer zones. In the study area, less than 1m to <8m thickness is noticed in the major part and 8 to 21m is noticed in the central part & a stretch in the eastern part of the study area. High layer thickness of >21 is observed as spots in the eastern part of the study area.**

***Keywords*: Resistivity survey, Ground water.**

1. Introduction

Electrical resistivity technique for geophysical prospecting are entrenched and the most vital technique for groundwater investigation. The electrical resistivity method is one that has been broadly utilized in light of the hypothetical, operational and interpretational ease. The upsides of electrical methods additionally incorporate control over depth of investigation, portability of the equipment, accessibility of wide range of simple and neat interpretation techniques, and the related software etc. Direct current (D.C.) resistivity (electrical resistivity) methods measure earth resistivity by driving a D.C. motion into the ground and measuring the subsequent potentials (voltages) created in the earth. From the information acquired, the electrical properties of the earth (the geoelectric section) can be inferred. Thusly, from those electrical properties we can derive the geological feature of the earth.

In geophysical and geotechnical narrative, the expressions "electrical resistivity" and "D.C. resistivity" are utilized synonymously. A few geographical parameters which influence earth resistivity (and its reciprocal, conductivity) incorporate clay substance, soil or formation porosity and scale of water saturation.

The theory and routine with regards to these methods for groundwater investigations is well recognized by Bhattacharya and Patra (1968) and Parasinis (1973). The interpretation of resistivity data and its application to groundwater study about has been given in detail by Zohdy (1965 and 1975). D.C resistivity methods might be utilized as a part of the profiling mode (Wenner surveys) to guide parallel changes and recognize near-vertical elements or they might be utilized as a part of the sounding mode (Schlumberger array) to decide depth to geoelectric horizons (Ex. depth to water table). Both profiling and vertical electrical sounding (VES) has been effectively connected to different geological formations by (Flathe 1955, Zohdy et al. 1974). Basic uses of the D.C resistivity technique incorporate delineation of collective deposits for quarry operations, approximate depth to water table and bedrock or to other geoelectric margins and detecting other geologic features (Verma et al. 1980).

2. Study Area

The vellar river basin originates from shavraiyan hills and its flow towards of salem, Perambalur and Cuddalore in the northern part of Tamilnadu which draining the near Parangipettai into Bay of Bengal. An approximately, total length of the vellar river is about 150 km, and its total area of basin 2520 Sq.km. The vellar river basin is located on northern part of Tamilnadu, southern India and between the latitudes 11o 13'N -12o 00' N and longitude 78o 13'E -79o 47'E. This basin is streams flow between the Ponnaiar, Paravanar and Cauvery river basins and the topography lying on Kalrayan hills, Attur Taluk of Salem District is drained by river upper vellar, Vasista Nadhi known as upper Vellar joined with to form the Vellar in the Perambalur Taluk of Permabalur District.

3. Methodology

A. Interpretation Procedures

1) Vertical electrical sounding (VES)

There are four basic category of sounding curve depending on the resistivity allocation with depth. If ρ^1, ρ^2 andρ^3 are the resistivity of the subsurface layers with ρ^1at the top followed by ρ^2 andρ^3.

i. $\rho1<\rho2<\rho3$ is defined as A-type
ii. $\rho1<\rho2>\rho3$ is defined as K-type
iii. $\rho1>\rho2<\rho3$ is defined as H-type
iv. $\rho1>\rho2>\rho3$ is defined as Q-type

*Corresponding author: raadhansuresh@gmail.com

The VES information was analysed at first with the curve coordinating utilizing different master curve manuals (Stefenesco 1930, Orellana and Mooney 1966, Rijkswaterstatt 1969) for acquiring the underlying models. Iterative inversion algorithms created by Gupta Sarma, (1982), Zohdy (1974) are accessible utilizing diverse inversion codes. The sounding curves were interpreted utilizing the software IP2WIN (Vender Velpan 1988) a program based on the steepest upright method. Table 2 gives the interpreted layer parameters (layer thickness and electrical resistivity) of 50 VES. Run of the mill sounding curves acquired in the study area, are shown in Figure 1. The curves indicates maximum of two layers. The maximum depth of data of 79.81 m is gotten at VES 42. Dominant part of the sounding curves are found as "K" type and then "A". In view of the VES locations VES Profile is prepared covering the VES locations from north east to southwest in the study area.

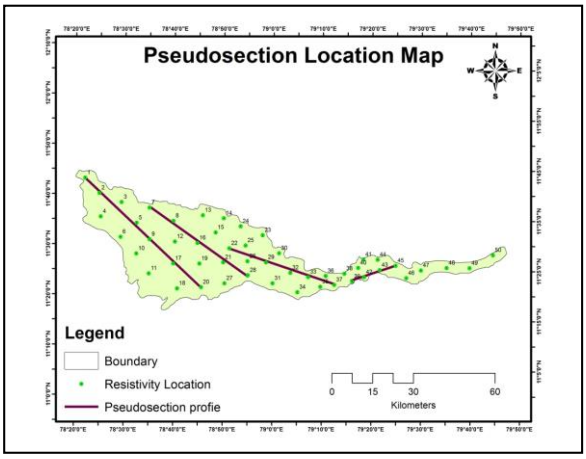

Fig. 1. Location map of the study area

2) Electrical Resistivity Method

In resistivity technique for electrical prospecting, an electric field is unnaturally made in the ground by methods for either galvanic batteries (DC) or low frequency AC generators. Electrical resistivity is characterized as the resistance offered by a unit cube of material for the flow of current through its normal surface. On the off chance that "L" is the length of the conductor and "A" is its cross-sectional zone, then the resistance (R) is characterized as

$$R=\rho L/A$$

In MKS system the unit of resistivity is Ohm-meter (W-m). The reciprocal of resistivity is called conductivity and denoted by σ, the unit of conductivity is mho/meter.

3) Apparent resistivity

The homogeneous and isotropic directing medium ρ is independent of the position of electrodes on the surface and electrodes organisation while measuring the potential distinction between any two point in a four-electrode array containing a couple of present and potential electrodes. The apparent resistivity of geologic formation is equivalent to the true resistivity of made up homogeneous and isotropic medium in which, for a given electrode configuration and current strength, I, the calculated potential differentiation ΔV is equivalent to that for the given heterogeneous and anisotropic medium. The apparent resistivity depends upon the geometry and resistivity of the element constituting the given geologic medium.

$$\rho a = K\,(\Delta V/I)$$

Where K, is the geometrical variable having the measurement of length (m). Resistivity of rock formations vary over a wide range, depending upon mineral constituents of rock, density, porosity, pore size and shape, water content, quality of water and temperature. There is no fixed limit for resistivity of different rocks, igneous and metamorphic rocks yield value in the scope of 102 to 108 Ohm m, sedimentary and unconsolidated rocks are different between 1 to 104 Ohm m.

4) Resistivity measurements

The most part, to measure the resistivity's of the subsurface formation, four electrodes specifically two current electrodes A and B and two potential electrodes M and N are essential. There are different electrodes arrangements for measuring the potential differentiation, which are individually utilized for various purposes in exploration techniques (Keller and Frishknecht, 1966). The most well-known among them are Wenner (1915) and Schlumberger (1920).

5) Schlumberger array

The Schlumberger array, comprise of four co-linear point electrodes to measure the potential inclination at the midpoint. In this array, the current electrodes and potential electrodes are spaced in the ratio of 1:5 and the geometrical variable K for this exhibit is given by,

$$K = \pi\,\{(AB/2)^2 - (MN/2)^2\}/MN$$
$$\text{(i.e.) } K = \pi\,(s^2 - b^2)/2b$$

Apparent resistivity $\rho_a = K\,(\Delta V/I)$

Where, s = half spacing of current electrodes and b = half spacing of potential electrodes.

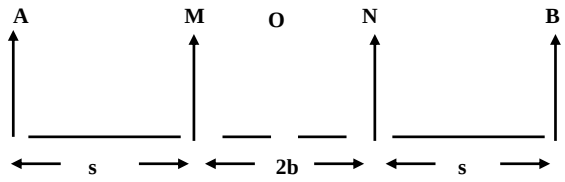

Where $s \geq 5b$

The above sketch is the schematic representation of Schlumberger electrode configuration, when AM = MN = NB = s, results the Wenner configuration.

6) Electrode configuration for the present study

In the present work, the field study has been carried out using Schlumberger configuration to measure apparent resistivity. Vertical electrical soundings have been conducted at 50 locations of this sub basin using SSR-MP-ATS model resistivity meter. The apparent resistivity was interpreted using IPI2win software to obtain the true resistivity and layer thickness of the sub surface formation. Besides, iso-resistivity and iso-layer thickness spatial maps were generated at different

AB/2 spacing using the field apparent resistivity data. Besides, for better understanding the subsurface lithological variation and delineate potential groundwater zones, an attempt has been made to prepare resistivity pseudo sections of the study area.

4. Results and Discussions

Four profiles were made from north-west to south - east direction (Figure 1). In the first profile VES-1, 2, 5, 9, 17 and 20 are considered for construction of pseudo section as shown in Figure 2 where the overall resistivity varied from less than 3 Ω-m to nearly 2.68 Ω-m. It is observed that resistivity is gradually increased from the top layer to bottom layer and resistivity in the top layer is varied from less than 1.2 Ω-m to 13 Ω-m. The top layer noted up to 10m from the ground level in the southern side and decreased to less than 1 m in the middle whereas in the northern side it is observed up to 3 m. Below the top layer, resistivity range of 13 to 72 Ω-m is observed as a second layer and the third layer found with resistivity range of 72 to 223 Ω-m.

The second profile pseudo section constructed using VES-7, 8,16,21,28 where it observed the similar layer structure and pattern of profile-1. However, the resistivity range varied from less than 0.5 Ω-m to above 2343 Ω-m. The pseudo section of the profile-2 is shown in Figure 3.

In the third profile, VES-22, 29, 32, 33 and 37 are considered for pseudo section the overall resistivity varied from less than 0.7 Ω-m to above 722 Ω-m. Resistivity of less than 3 Ω-m was found as the top layer from surface and below resistivity range of 0.75 to 19.3 Ω-m is observed. The resistivity gradually increased up to 722 Ω-m in the third layer and in fourth layer, it increased further up to 0.75 Ω-m. The top layer thickness is comparatively high in the middle part where as it is less in either side. The same layer structure and pattern are not exactly followed in the bottom layers and in the northern side resistivity of 25 to 139 and above 139 Ω-m is represented. The pseudo section of the profile-3 is shown in Figure 4.

In the fourth profile VES-39, 42, 43 and 45 are considered for pseudo section and it is shown in Figure 5.4. It is observed that low resistivity of less than 1.23 Ω-m was noticed as the top layer in the middle and southern part whereas the resistivity range of 14 Ω-m to 37.3 Ω-m was noticed in the norther part. The resistivity range of 38 to 68 Ω-m is observed as a second layer in the southern part, and it increased further to 51.8 Ω-m in the third layer. The fourth layer resistivity varied from 89 to 100 Ω-m in the southern side, and it has become a top layer in the northern side.

A. VES curve types

The nature of VES curve depends on the geological and hydrogeological situation and the maximum electrode spread is employed. Qualitative interpretation is also attempted by preparing a spatial variation map showing the types of curves encountered. Such maps can clearly indicate the disposition of different resistivity zones with depths. In the present study A, K and KH- type curves are seen in most of the places of the study area and the obtained sounding curves types is shown in Table 1. The presence of a highly resistive top soil and limited saturated aquifer zone with a resistive substratum is indicated by this type of curve. The spatial map of the curves types are shown figures 6 to 9.

Table 1
Curve types

Curve Types	VES Locations
A	1,4,6,9,10,13,16,17,32,41,42,48
K	2,3,7,11,12,14,19,21,22,23,25,26,27,33,34,36,37,38,39,40,43,45
H	5,18,24,28,35
KH	7,15,31,44,47,49,50
Q	20,30
KQ	46

B. Geoelectrical layers

The VES data of the study area has been interpreted through curve matching technique using IPI2Win software version 3.0.1.a (Moscow State University 1990-2003) and the interpreted sounding curves are given in the Figure 12. The layer wise aquifer thickness and resistivity's obtained are listed in Table 2.

The interpreted true resistivity represented 3-layer curve types in many locations and 4 layer curves are also obtained few locations. Besides, over all resistivity varied from less than 1 Ω-m to 2343 Ω-m and the RMS error percent varied from 4 to 10. The RMS error percent was obtained less than 10 in all locations.

The first layer resistivity varied from 1.5 to 10.2 where low resistivity found in VES locations 1, 12 and 37 and high resistivity found in VES location 20. The layer thickness of first layer found less as 1m in few VES location and high thickness of 8 m was noticed in VES location 13. In order to understand the resistivity and layer thickness variation of the study area, spatial map has been prepared for the same as shown in Figure 6.

The very low resistivity of less than 1.5 is noticed in the eastern part and small patches along the central boundary of the study area. The resistivity range of 10 to 20 is observed in the central part and resistivity range of 20 to 60 is noticed in the west and north western part. In a small patch is observed with the resistivity range of 60 to 140 in the north eastern part of the study area. The total thickness of the first layer varied from less than 1m to more than 8.19 m. The layer thickness is varied from 1m to 1.5 to 2 m in the central and western part of the study area whereas in the eastern central part, particularly in north eastern side observed more than 2m.

In the second layer, low resistivity of less than 1 Ω-m was noted in VES-35 and the higher resistivity value of 2343 was observed in VES-29. Less layer thickness of less than 0.5m has been indicated in VES-47 and high layer thickness of 66m was noted in VES-48. The spatial variation of second layer resistivity is shown in Figure 9. The resistivity range of >45 Ω-m has been noticed as small patches in the east and western part of the study area whereas 45-235 Ω-m and >235 was noticed as major part and found as patches in the western part. The layer thickness of <7 m was observed in most of the study area whereas 7 – 20m is noticed in the western and eastern part and high thickness of >20m is observed in the patches. The layer

thickness variation is shown in Figure 9.

A very low resistivity value of less than 0.74 Ω-m of the third layer was observed in VES location 49. The high resistivity value of 722 Ω-m was noted in VES location 28. The low resistivity of less than 36 Ω-m was noticed in major part of the study area. The resistivity range of 36 -370 Ω-m and >370 Ω-m were noticed around the low resistivity range in the central part whereas resistivity range of 60 to 120 Ω-m was noticed as small spots in the central part represented. The resistivity range of >370 Ω-m was observed as patches in central part of the study area. The spatial variation of resistivity in the third layer is shown in Figure 10.

In the study area, less than 1m thickness is noticed in the major part and the thickness < 8 m. Layer thickness of 8 to 21m is noticed in the central part and a stretch in the eastern part of the study area. High layer thickness of >21 is observed as spots in the eastern part of the study area. The spatial map of the thickness of third layer is shown in Figure 11.

Table 1
Interpreted layer parameters from geoelectric resistivity soundings of the study area. ρ, h and H are electrical resistivity (Ohm-m), layer thickness (m), and total thickness (m) respectively. Suffixes indicate the layer number

VES	ρ_1 (ohm-m)	ρ_2 (ohm-m)	ρ_3 (ohm-m)	ρ_4 (ohm-m)	h_1 (m)	h_2 (m)	h_3 (m)	H (m)	CURVE TYPE
1	7.09	53.70			1.13	18.70		19.83	A
2	11.50	239.00	10.90		1.09	0.87	3.41	5.37	K
3	14.70	241.00	18.80		0.96	0.96	7.37	9.29	K
4	16.90	76.50			2.01	16.20		18.21	A
5	5.84	0.73	4.84		1.51	1.88	19.40	22.79	H
6	10.60	57.10			0.61	12.80		13.41	A
7	8.87	796.00	20.80		2.44	4.00	16.60	23.04	K
8	8.37	32.30	4.56	87.40	1.43	1.73	3.36	6.52	KH
9	2.07	26.20			2.06	29.50		31.56	A
10	10.40	95.60			0.68	21.30		21.98	A
11	12.10	587.00	9.21		1.00	0.60	3.52	5.12	K
12	3.79	17.30	1.45	6.60	0.71	1.15	2.26	4.12	K
13	18.00	26.40			8.19	9.19		17.38	A
14	29.70	170.00	55.00	2.43	1.24	2.33	16.20	19.77	K
15	4.84	33.00	3.07	16.30	1.48	1.63	4.10	7.21	KH
16	10.30	24.40			1.00	7.76		8.76	A
17	10.20	24.60			1.00	7.78		8.78	A
18	5.82	0.73	4.83		1.51	1.88	19.50	22.89	H
19	14.20	1283.00	9.62		1.00	0.12	3.71	4.83	K
20	223.00	21.00			2.53	24.70		27.23	Q
21	5.48	1.73	5.05		2.21	1.23	27.10	30.54	K
22	9.64	611.00	12.60		1.00	0.12	21.40	22.52	K
23	8.84	917.00	20.70		2.43	3.20	14.30	19.93	K
24	14.30	1.69	7.84		1.47	4.99	53.50	59.96	H
25	11.20	97.50	1.06		1.67	3.07	11.40	16.14	K
26	8.83	910.00	20.60		2.43	3.22	14.30	19.95	K
27	3.45	53.90	1.86		1.31	1.39	1.86	4.56	K
28	6.59	1.37	722.00		2.52	2.05	11.10	15.67	H
29	14.50	2343.00	10.10		1.00	0.24	3.86	5.10	K
30	12.50	4.07			2.40	11.20		13.60	Q
31	16.70	62.00	12.40	53.60	1.00	3.46	6.30	10.76	KH
32	5.75	7.83			1.06	16.60		17.66	A
33	13.20	737.00	9.47		1.00	0.23	3.60	4.83	K
34	5.66	13.50	1.57		2.42	2.19	5.40	10.01	K
35	5.36	0.57	543.00		2.15	3.24	6.13	11.52	H
36	20.20	220.00	7.78		1.00	0.38	2.71	4.09	K
37	1.20	3.28	1.16		1.00	3.90	3.69	8.59	K
38	7.42	2.25	184.00		1.04	6.61	14.10	21.75	K
39	13.00	246.00	14.70		1.00	8.42	7.55	16.97	K
40	9.67	88.60	2.54		1.67	1.60	3.87	7.14	K
41	4.21	8.04			1.00	37.60		38.60	A
42	4.41	8.36	20.70		1.51	13.50	64.80	79.81	A
43	49.00	227.00	7.53		1.56	1.40	6.91	9.87	K
44	40.20	841.00	13.80	89.80	1.00	0.25	2.20	3.45	KH
45	4.36	43.58	7.17		1.00	0.07	5.94	7.01	K
46	3.59	80.90	8.02	1.23	1.00	0.30	13.50	14.80	KQ
47	2.34	16.20	3.10	19.80	1.00	0.47	3.02	4.49	KH
48	2.63	6.61			1.00	66.50		67.50	A
49	1.21	28.40	0.73	31.80	1.00	0.91	3.08	4.99	KH
50	1.59	153.00	1.22	8.26	1.00	0.13	2.09	3.22	KH

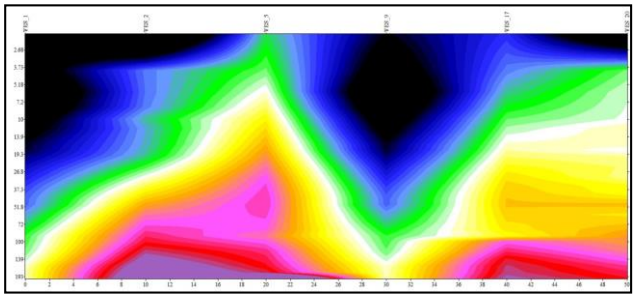

Fig. 2. Pseudo section profile 1

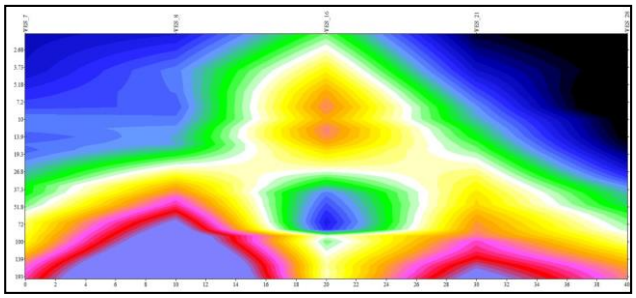

Fig. 3. Pseudo section profile 2

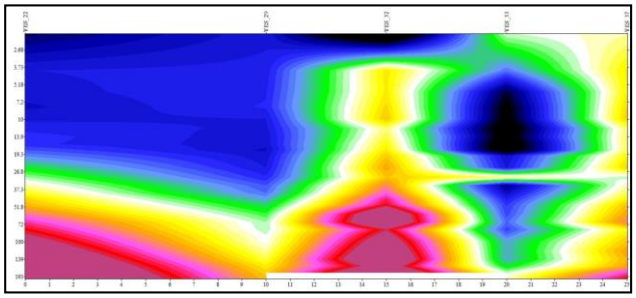

Fig. 4. Pseudo section profile 3

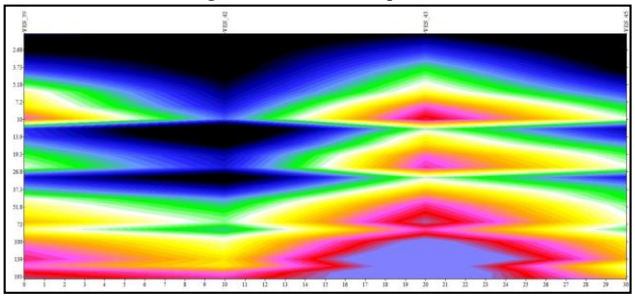

Fig. 5. Pseudo section profile 4

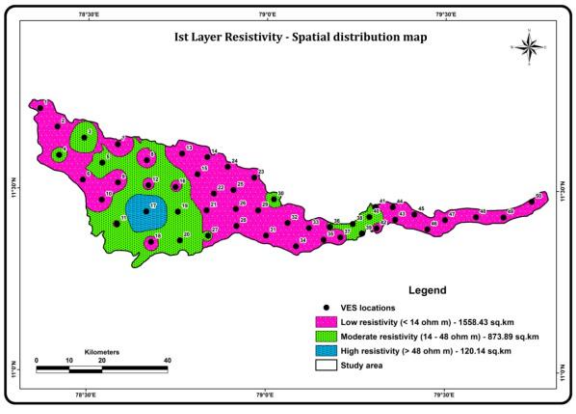

Fig. 6. Spatial distribution map of first layer resistivity

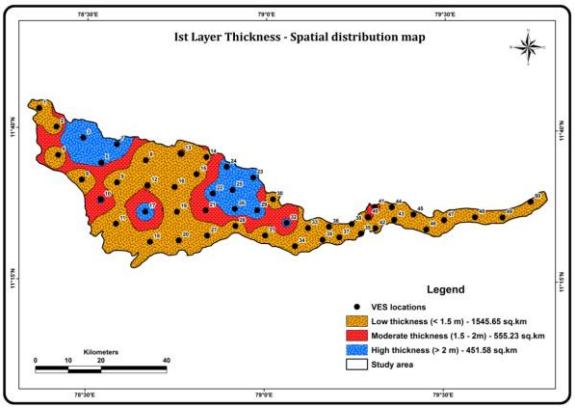

Fig. 7. Spatial distribution map of first layer thickness

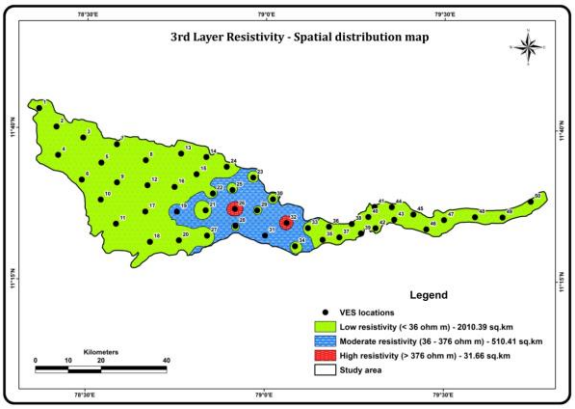

Fig. 8. Spatial distribution map of second layer resistivity

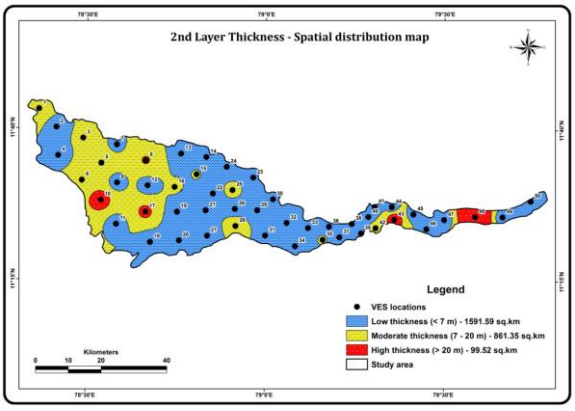

Fig. 9. Spatial distribution map of second layer thickness

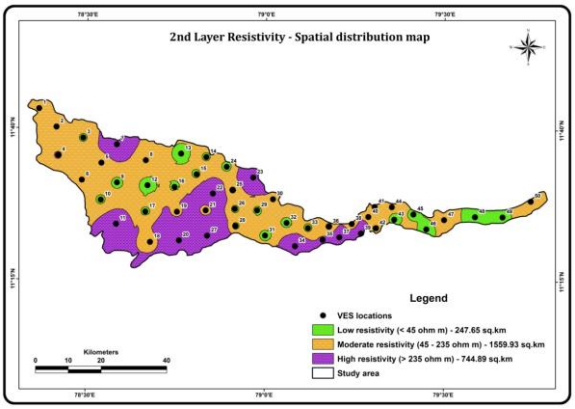

Fig. 10. Spatial distribution map of third layer resistivity

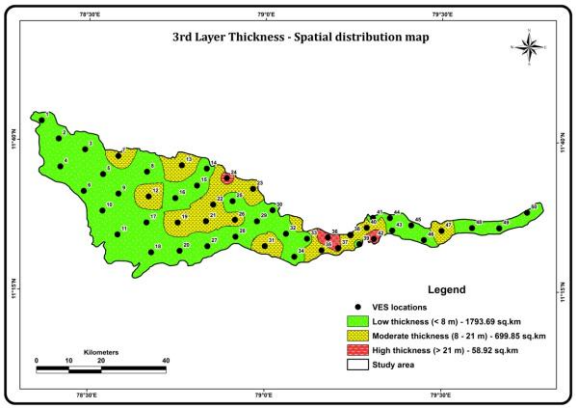

Fig. 11. Spatial distribution map of third layer thickness

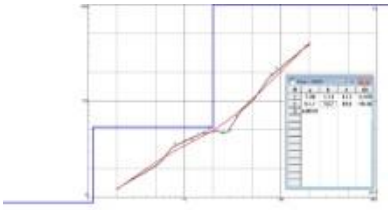

VES 1

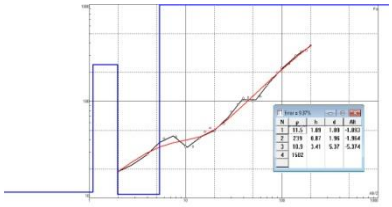

VES 2

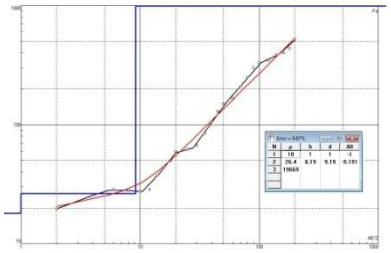

VES 3

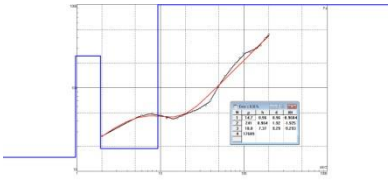

VES 4

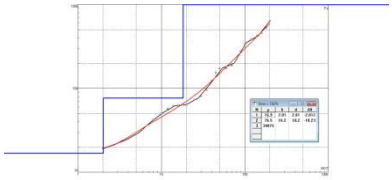

VES 5

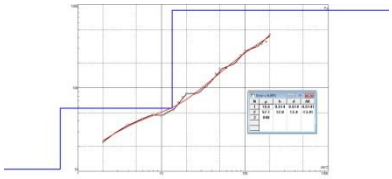

VES 6

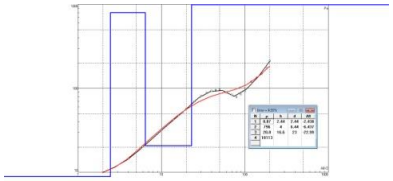

VES 7

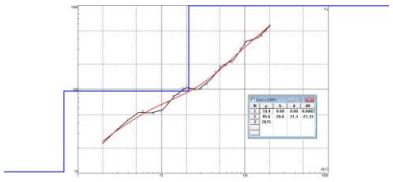

VES 8

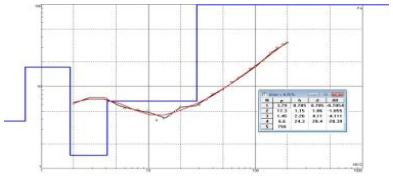

VES 9

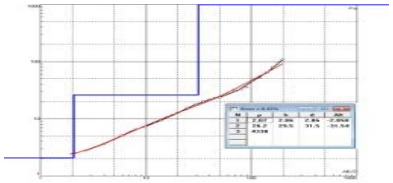

VES 10

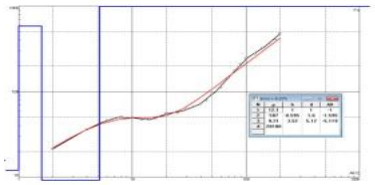

VES 11

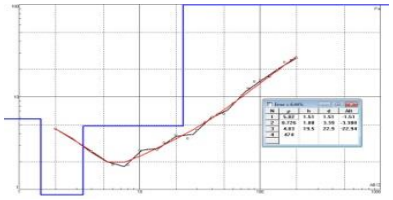

VES 12

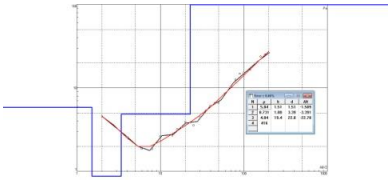

VES 13

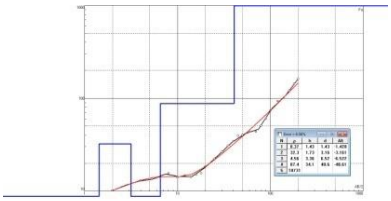

VES 14

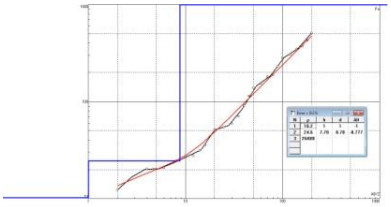

VES 15

VES 16

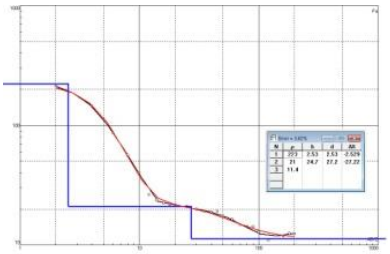

VES 17

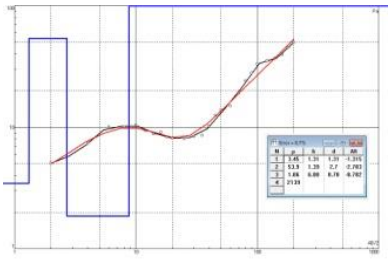

VES 18

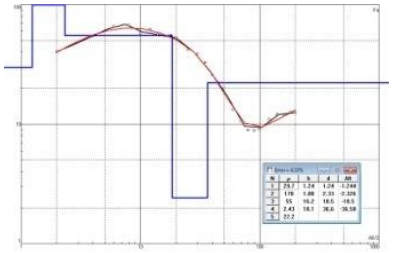

VES 19

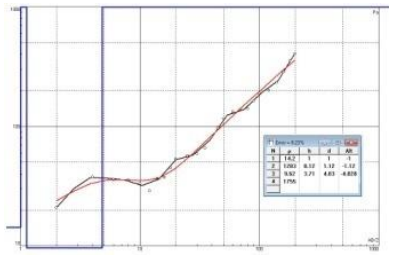

VES 20

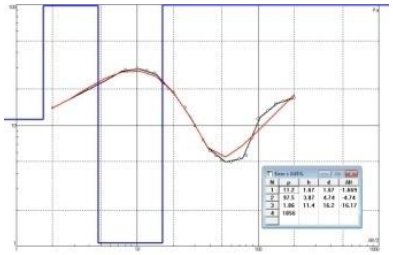

VES 21

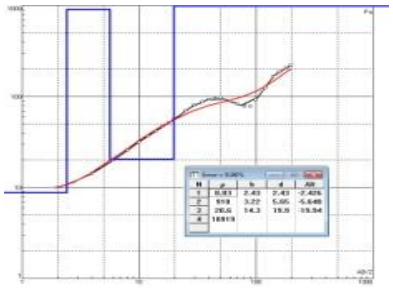

VES 22

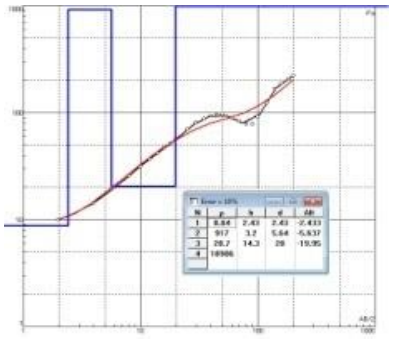

VES 23

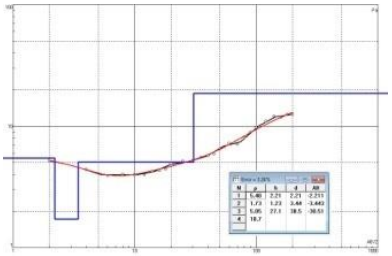

VES 24

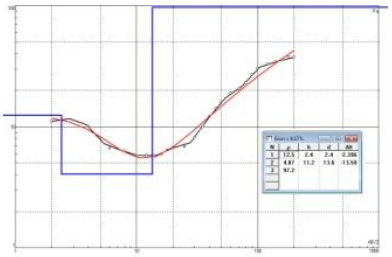

VES 25

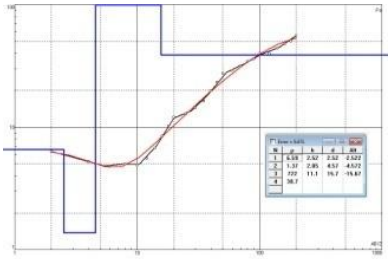

VES 26

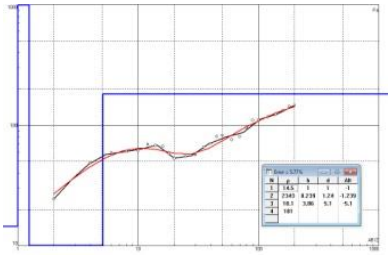

VES 27

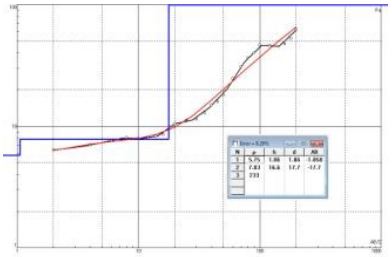

VES 28

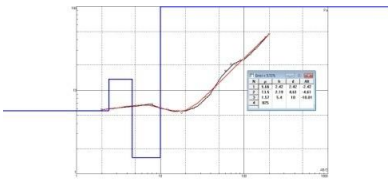

VES 29

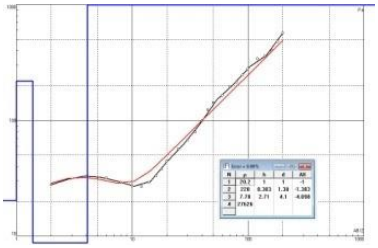

VES 30

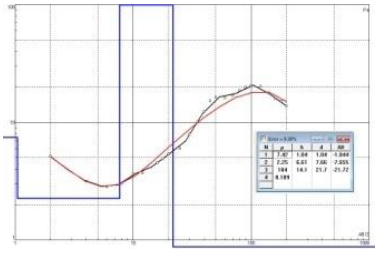

VES 31

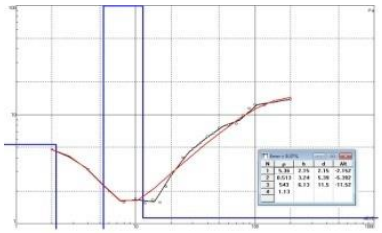

VES 32

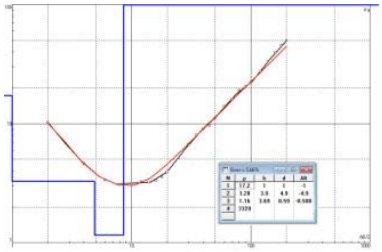

VES 33

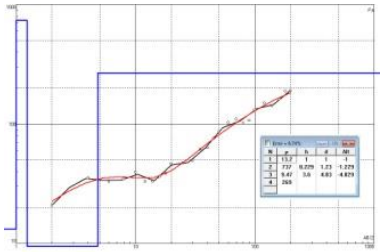

VES 34

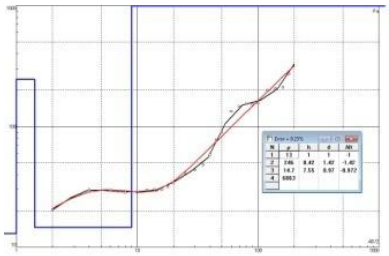

VES 35

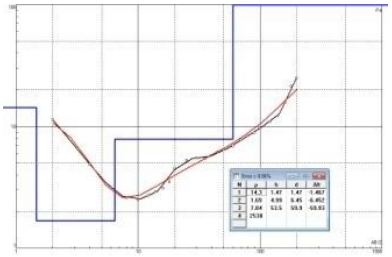

VES 36

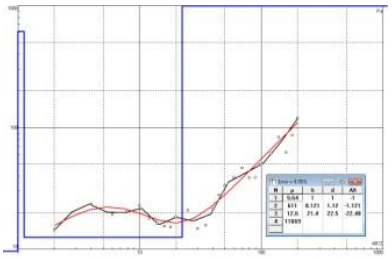

VES 37

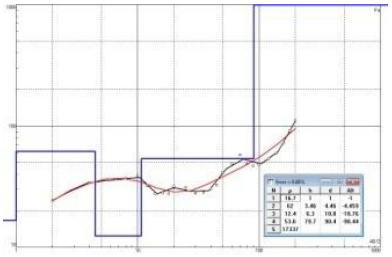

VES 38

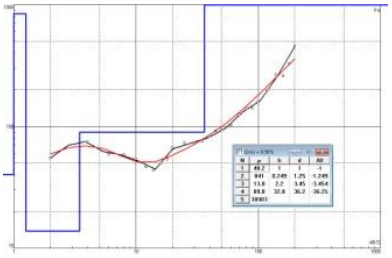

VES 39

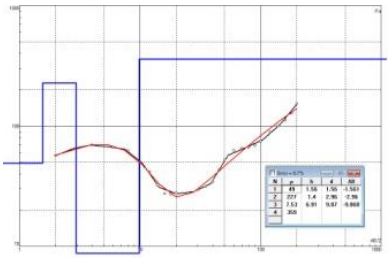

VES 40

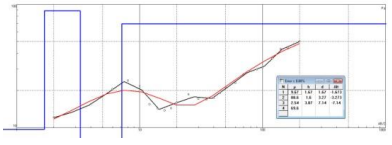

VES 41

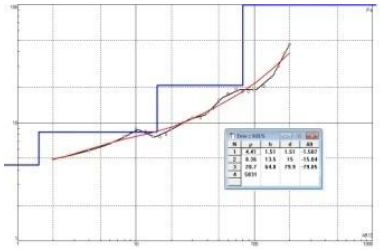

VES 42

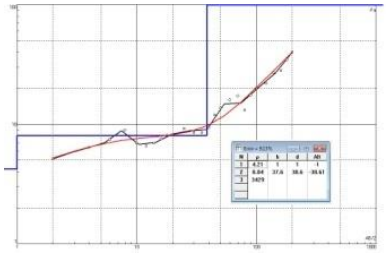

VES 43

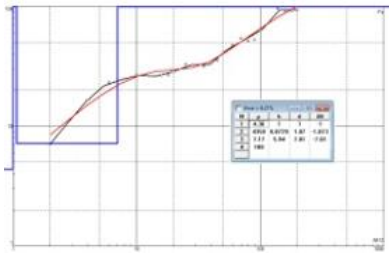

VES 44

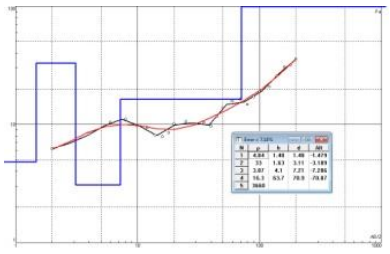

VES 45

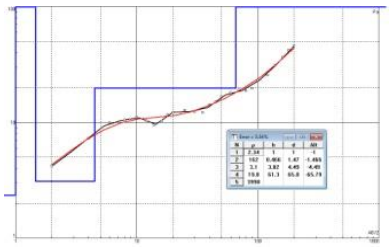

VES 46

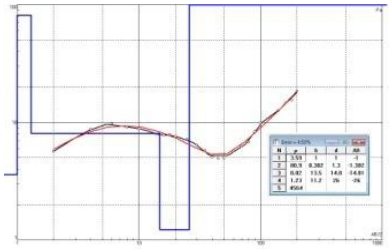

VES 47

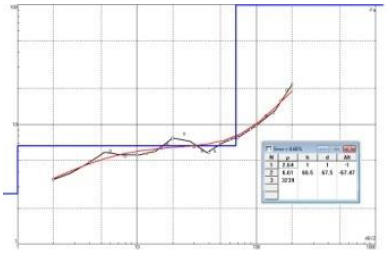

VES 48

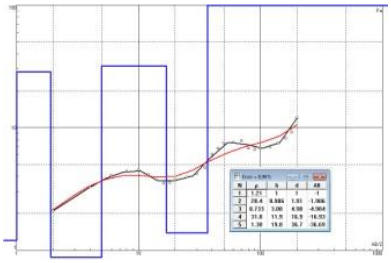

VES 49

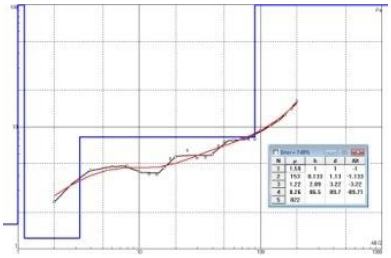

VES 50

Fig. 12. VES locations

5. Conclusion

The VES curves shows maximum of three layers and majority of the sounding curves are found as “K” type. The overall resistivity varied from less than 3 Ω-m to nearly 2.68 Ω-m. It is observed that resistivity is gradually increased from the top layer to bottom layer and resistivity in the top layer is varied from less than 1.2 Ω-m to 13 Ω-m. 3-layer curve types in many locations and 4 layer curves are also obtained few locations. The very low resistivity of less than 1.5 is noticed in the eastern part and small patches along the central boundary of the study area. In the second layer, low resistivity of less than 1 Ω-m was noted in VES-35 and the higher resistivity value of 2343 was observed in VES-29.

References

[1] Zohdy (1965 and 1975) Automatic interpretation of Schlumberger sounding curves, using modified Dar Zarrouk functions.

[2] Gupta sarma D. Computation of the time-domain response of a polarizable ground. Geophysics. 1982 Nov; 47 (11):1574-6.

[3] H. Flathe 1955 a practical method of calculating Geoelectrical model graphs for horizontally stratified media.

[4] Keller GV, Frischknecht FC. Electrical methods in geophysical prospecting. 1966.

[5] Orellana E, Mooney HM. Master Tables and Curves for Vertical Electrical Sounding Over Layered Structures; Tablas Y Curvas Patron Para Sondeos Electricos Verticales Sobre Terrenos Estratificados. Interciencia; 1966.

[6] P. K. Bhattacharya & H. P. Patra 1968. Direct Current Electric Sounding (Methods in Geochemistry and Geophysics, 9.) ix + 135 p., 47 figs., 16 tables. Elsevier Publishing Co., Amsterdam, London, New York. Price £3 15s.

[7] Rijkswaterstaat, the Netherlands. Standard graphs for resistivity prospecting. 1969.

[8] Roman P. Legocki Desh Pal S. Verma 1980 Identification of “nodule-specific” host proteins (nodulins) involved in the development of Rhizobium-Legume symbiosis.

[9] Stefanesco S, Schlumberger C, Schlumberger M. Sur la distribution électrique potentielle autour d'une prise de terre ponctuelle dans UN terrain à couches horizontales, homogènes ET isotropes. Journal de Physique ET le Radium. 1930 Apr 1; 1(4):132-40.

[10] V. Bhaskar Rao & B. V. Satyanarayana Murty (1973) Note on Parasnis' method for surface rock densities.

[11] Vender Velpen BP. A computer processing package for DC Resistivity interpretation for an IBM compatible. ITC J. 1988; 4:1-4.

[12] Wenner F. A method for measuring earth resistivity. Journal of the Washington Academy of Sciences. 1915 Oct 4; 5(16):561-3.

[13] Schlumberger C. Etude sur la prospection electrique du sous-sol. Gauthier-Villars; 1920.

[14] Zohdy AA, Eaton GP, Mabey DR. Application of Surface Geophysics to Ground-water Investigations: Techniques of Water Resources Investigations of the United States Geological Survey: Book 2: Collection of Environmental Data: Chapter. United States Department of the Interior; 1974.